A Change in the Light Curve of Kuiper Belt Contact Binary (139775) 2001 QG298

Lacerda, P. (2011). A Change in the Light Curve of Kuiper Belt Contact Binary (139775) 2001 QG298. Astronomical Journal, 142(3), 90. DOI: 10.1088/0004-6256/142/3/90

Published in:
Astronomical Journal

Document Version:
Peer reviewed version

Accepted, 18 July 2011

A Change in the Lightcurve of Kuiper Belt Contact Binary (139775) 2001 QG_{298}

Pedro Lacerda

Astrophysics Research Centre, Queen's University Belfast, Belfast BT7 1NN, UK

p.lacerda@qub.ac.uk

ABSTRACT

New observations show that the lightcurve of Kuiper belt contact binary (139775) 2001 QG_{298} has changed substantially since the first observations in 2003. The 2010 lightcurve has a peak-to-peak photometric of range $\Delta m_{2010} = 0.7 \pm 0.1$ mag, significantly lower than in 2003, $\Delta m_{2003} = 1.14 \pm 0.04$ mag. This change is most simply interpreted if 2001 QG_{298} has an obliquity near 90°. The observed decrease in Δm is caused by a change in viewing geometry, from equator-on in 2003 to nearly 16° (the orbital angular distance covered by the object between the observations) off the equator in 2010. The 2003 and 2010 lightcurves have the same rotation period and appear in phase when shifted by an integer number of full rotations, also consistent with high obliquity. Based on the new 2010 lightcurve data, we find that 2001 QG_{298} has an obliquity $\varepsilon = 90° \pm 30°$. Current estimates of the intrinsic fraction of contact binaries in the Kuiper belt are debiased assuming that these objects have randomly oriented spins. If, as 2001 QG_{298}, KBO contact binaries tend to have large obliquities, a larger correction is required. As a result, the abundance of contact binaries may be larger than previously believed.

Subject headings: Kuiper belt: general — Kuiper belt objects: individual (2001 QG_{298}) — methods: data analysis — techniques: photometric

1. Introduction

Located approximately between 30 and 50 AU from the Sun, the Kuiper belt represents the outer frontier of the currently observable solar system. The belt is estimated to hold

roughly forty thousand objects larger than 100 km in diameter (Jewitt & Luu 1995; Trujillo et al. 2001; Bernstein et al. 2004; Fuentes & Holman 2008; Fraser et al. 2008). More than one thousand objects have been detected but only six hundred have multi-opposition observations and well-determined orbits. The Kuiper belt objects (KBOs) are remnants of outer solar system planetesimals and their study may shed light on the complex process that led to the formation of planets. Our understanding of the physical properties of KBOs remains rudimentary as most are too faint for detailed investigation.

Many KBOs are binary. Among the dynamically cold, "classical" population (low eccentricity and inclination KBOs located between the 3:2 and the 2:1 mean-motion resonances with Neptune, at 39.4 and 47.8 AU) the binary frequency is inferred to be ∼20% whereas in other dynamical subsets the fraction is lower, at 5 to 10% (Stephens & Noll 2006; Noll et al. 2008). Binaries probably formed early on (Weidenschilling 2002), before the Kuiper belt lost more than 99% of its original mass (Kenyon & Luu 1998; Booth et al. 2009), because the current-day number density of KBOs is too low for frequent pair encounters. It is also possible that planetesimals formed in clusters of two or more bodies and that the binaries we see today are direct remnants of that process (Nesvorný et al. 2010). Thus, binaries are particularly useful probes of the conditions under which planetesimals formed. For instance, the symmetry in surface properties of KBO pairs argues for a chemically homogeneous formation environment (Benecchi et al. 2009). But the current binary abundance also bears record of the effects of collisional and dynamical processes that have eroded the original population (Petit & Mousis 2004). It is highly desirable to find ways to isolate the effects of formation, evolution, and erosion. The relative frequency of binaries within different regions of the Kuiper belt, and their distributions of orbital properties and relative mass of the components are quantities that should be sought to help clarify the formation and evolution of binaries (Schlichting & Sari 2008b; Murray-Clay & Schlichting 2011; Nesvorný et al. 2011).

Most known binaries are resolved (physical separations >1500 km; Noll et al. 2002; Stephens & Noll 2006; Stansberry et al. 2006; Grundy et al. 2011). The exception is the 500 km × 175 km contact binary (139775) 2001 QG_{298}, identified from analysis of its rotational lightcurve (Figure 1; Sheppard & Jewitt 2004, hereafter SJ04). Using time-resolved measurements taken mainly during 2003, the authors found that 2001 QG_{298} displayed extreme photometric variability ($\Delta m \sim 1.2$ mag) and a relatively slow rotation period ($P \sim 13.77$ hr). The large photometric range, caused by the eclipsing nature of the binary, exceeds the $\Delta m = 0.75$ mag produced by two spheres in contact (axis ratio $b/a = 0.5$) because the contact binary components are tidally elongated along the line connecting the centers (Weidenschilling 1980; Leone et al. 1984). The large Δm found for 2001 QG_{298} also implies that the system was observed almost equatorially in 2003. Models of 2001 QG_{298}'s lightcurve based on figures of hydrostatic equilibrium lend strong support to these assertions (Taka-

hashi & Ip 2004; Lacerda & Jewitt 2007; Gnat & Sari 2010) and allow the bulk density of $2001\,QG_{298}$ to be estimated at $\rho = 0.59^{+0.14}_{-0.05}$ g cm^{-3}. This surprisingly low density implies that $2001\,QG_{298}$ is mostly icy in composition and is significantly porous.

The example of $2001\,QG_{298}$ suggests that between 10% and 20% of KBOs could be contact binaries, depending on surface scattering properties (SJ04; Lacerda & Jewitt 2007). This high fraction is consistent with the observation that the frequency of resolved binaries increases dramatically with decreasing orbital separation (Kern & Elliot 2006). However, despite their high abundance, contact binary KBOs remain elusive. The reason is that these objects are unresolved and can only be identified if they happen to be nearly equator-on. The consequence is that as many as 85% of contact binaries may go unnoticed due to unfavorable observing geometry. High phase angle observations that have been shown to increase the chance of detecting contact binaries (Lacerda 2008) can not be applied to the distant KBOs as their phase angles remain below 2° when observed from Earth. Interestingly, the Jupiter Trojans also contain a fairly large fraction of contact binaries, comparable to that found for KBOs. In addition to the well-known case of (624) Hektor (Hartmann & Cruikshank 1978; Detal et al. 1994; Cruikshank et al. 2001; Lacerda & Jewitt 2007), two other contact binaries have been identified in a survey of 114 Trojans (Mann et al. 2007). When corrected by the probability of observing these objects close to equator-on, Mann et al. (2007) find an intrinsic contact-binary fraction of at least 6% to 10%. The apparently high abundance of contact binaries and the prospect of measuring their densities makes these primitive objects particularly interesting targets of study.

QG_{298} has travelled a significant angular distance ($\sim 16°$) in its heliocentric orbit since the first observations in 2003. In this paper we compare new 2010 lightcurve data with the SJ04 observations and make inferences on the obliquity of $2001\,QG_{298}$. In Section 2 we describe our observations, in Section 3 we report our findings on the lightcurve and obliquity of $2001\,QG_{298}$, in Section 4 we discuss the implications of our findings for the abundance of contact binaries, and in Section 5 we present our conclusions.

2. Observations

Visible-light observations were taken at the 2.5-m Isaac Newton Telescope (INT) operating on the island of La Palma in the Canary Islands, Spain. The INT was equipped with the Wide Field Camera (WFC), mounted at the f/3.29 prime focus. The WFC consists of an array of 4 thinned EEV 4K×2K charge-coupled devices (CCDs). The CCDs have an image scale of 0.33 arcsec per pixel and the full array covers approximately 34 arcmin squared on the sky. Our observations made use of CCD #4 which is the most central with respect to

the field of view. Details of the observing times and conditions can be found in Table 1.

Our target, 2001 QG_{298}, was observed through the Sloan-Gunn r filter (Isaac Newton Group filter #214) which approximates the r band in the Sloan Digital Sky Survey (SDSS) photometric system. Consecutive 600 s exposures were obtained in a consistent manner to measure variations in the brightness of QG_{298}. The rate of motion of 2001 QG_{298} across the sky was <2.32 arcsec/hr (0.39 arcsec in 10 minutes) keeping it well within the seeing disc during the observations. All frames were bias-subtracted and flat-fielded using the median of a set of dithered exposures taken during twilight. In the reduced images, the brightness variations of 2001 QG_{298} were measured differentially against 8 bright, not saturated, field stars to offer protection from fluctuations in atmospheric transmission and seeing. The mutual relative photometry of the comparison stars is stable to better than ± 0.01 mag throughout all the observations. The field containing 2001 QG_{298} (RA = $0^{\rm h}.838$, dec = $1^{\circ}.964$) at the time of our observations is included in the SDSS photometric catalog. This allowed us to absolutely calibrate our observations directly against SDSS magnitudes of 5 of the 8 comparison stars (see Table 2) chosen for their spatial distribution and exceptional photometric stability.

3. Results

3.1. The lightcurve of 2001 QG_{298}

We used our photometric measurements of 2001 QG_{298} to construct a lightcurve (magnitudes versus time) for this object. Figure 2 shows how our 2010 lightcurve and the SJ04 lightcurve compare. Overall, the lightcurves have the same period and appear aligned in rotational phase. The 2010 photometric range is smaller by about 0.5 magnitudes.

The apparent alignment in rotational phase between the 2003 and 2010 lightcurves is real. All times were measured relative to 2010 Aug 13 at 0h UT (zero rotational phase) and then phased to the period $P = 13.7744 \pm 0.0002$ hr (SJ04). The maximum light-travel time difference between any two measurements included in the 2003 and 2010 lightcurves is less than 1.5 minutes (0.002 rotations) so no delay correction was required. More importantly, the relative uncertainty in the rotational period of 2001 QG_{298} translates to an uncertainty of 0.06 rotations between the 2003 and 2010 data. The latter implies that the phase alignment in Figure 2 is accurate to ± 0.06 in rotational phase.

The vertical axis in Figure 2 indicates magnitudes relative to the maximum apparent brightness of 2001 QG_{298}. The vertical alignment of the 2003 and 2010 data is artificially set to facilitate comparison of the photometric ranges in 2003 and 2010 (Δm_{2003} and Δm_{2010}). In

our data, we find that at maximum brightness 2001 QG_{298} has magnitude $m_r = 21.63 \pm 0.02$ mag. This measurement is absolutely calibrated using SDSS catalog stars as described in Section 2 and the error is dominated by uncertainties in the r magnitudes of the calibration stars (Table 2). SJ04 found that at maximum brightness 2001 QG_{298} has an absolute magnitude $m_R(1, 1, 0) = 6.28 \pm 0.02$ mag. The expected apparent magnitude at the time of our observations is thus

$$m_R(R, \Delta, \alpha) = m_R(1, 1, 0) + 5 \log R\Delta + \beta\alpha = 21.46 \pm 0.04 \text{ mag},$$

where R, Δ and α are taken from Table 1, and $\beta = 0.15 \pm 0.01$ mag/° is the phase coefficient for KBOs (Sheppard & Jewitt 2002). To compare the expected m_R magnitude with our new m_r measurement we used two approaches. Firstly, we converted our SDSS r magnitude to a Cousins R magnitude using the transformation equations in Smith et al. (2002) and the broadband colors of 2001 QG_{298} ($B - V = 1.00 \pm 0.04$ mag and $V - R = 0.60 \pm 0.02$ mag; see SJ04): we obtain an equivalent R magnitude $m_R = 21.36 \pm 0.04$ mag. Secondly, we took the transmission profiles of the two filters (available from the Isaac Newton Group online filter database) and convolved each with the spectrum of 2001 QG_{298} to find an integrated flux ratio 1.215. This corresponds to magnitude difference $m_r - m_R = 0.21$ mag between the filters. Subtracting that difference from our m_r measurement we obtain an equivalent R magnitude $m_R = 21.42 \pm 0.04$ mag. We assumed the spectrum of 2001 QG_{298} to be linear with a slope 22.6% $(1000\text{Å})^{-1}$, as calculated from the object's $B - V$ color. Although both approaches are uncertain, they agree at the 1-σ level and fall within 0.1 mag of the expected apparent magnitude based on the object's absolute magnitude and geometric circumstances.

3.2. The obliquity of 2001 QG_{298}

Between the time of the SJ04 observations in 2003 and the time of our 2010 observations 2001 QG_{298} has travelled 16° along its heliocentric orbit. A diagram of the geometric circumstances of the two sets of observations is shown in Figure 3. The change in observing geometry between 2003 and 2010 has predictable effects on the lightcurve of 2001 QG_{298}. Given the extreme variability displayed in 2003, 2001 QG_{298} was probably observed equator-on, i.e. at aspect angle (measured between the line of sight and the spin pole) $\theta_{2003} \sim 90°$ (Figure 3). This assertion is backed by detailed models of the 2003 lightcurve based on figures of hydrostatic equilibrium (Takahashi & Ip 2004; Lacerda & Jewitt 2007; Gnat & Sari 2010). Those simulations consider close and contact binaries in which the components are homogeneous and strengthless, and orbit each other in tidally locked, circular orbits. Under these conditions, the binary components assume shapes that balance gravitational

(including mutual tidal) and rotational accelerations. Furthermore, the exact shapes of the binary components, their mutual orbit period (≡ spin period), and their density are all interdependent. The practical result is that the density can be inferred from the spin period and the component shapes. The simulations search the space of hydrostatic equilibrium binary solutions and orientations (aspect angles) for the combination that best fits the observed lightcurve and then use the spin period to extract the density. This technique has been tested on the observationally well-characterized Jovian Trojan contact binary (624) Hektor (Lacerda & Jewitt 2007), using observations at multiple geometries along its 12-yr orbit (Dunlap & Gehrels 1969).

In the case of $2001\,QG_{298}$, all attempts to simulate the SJ04 lightcurve yield equivalent results and agree upon a nearly equator-on geometry, and a low bulk density $\rho \sim 0.6 - 0.7$ g/cm^{-3} (Takahashi & Ip 2004; Lacerda & Jewitt 2007; Gnat & Sari 2010). For our purposes, we will use the models of $2001\,QG_{298}$ found by Lacerda & Jewitt (2007, hereafter LJ07); the SJ04 data and respective LJ07 model lightcurves are shown in Figure 1. The binary models are rendered in Figure 4. LJ07 make use of the Roche approximation which calculates the deformations on each component independently, assuming the other component's mass is concentrated on a point (Chandrasekhar 1963; Leone et al. 1984). In the Roche binary approximation the binary is composed of two triaxial ellipsoids described by their axis ratios, their mass ratio, and their orbital separation. LJ07 include the effects of limb darkening when simulating the Roche binary lightcurve. They consider two extreme light scattering laws: a lunar-type (Lommel-Seeliger or backscatter reflection) law, appropriate for low albedo, rocky surfaces, and an icy-type (Lambertian or diffuse reflection) law, suitable for high albedo surfaces. The lunar law leads to negligible limb darkening and so generates symmetric lightcurves for which both mutual eclipses produce the same signature. The icy law causes considerable limb darkening and so produces asymmetric lightcurves if the binary components have different masses/sizes. The SJ04 hints at a slight difference between the two lightcurve minima (Figure 1), intermediate to the extreme lunar and icy cases, so LJ07 identify two models, one for each scattering law, that bracket the data (see Figure 1). The model parameters are listed in Table 3.

We want to investigate how the lightcurve is predicted to change between 2003 and 2010 depending on the binary's obliquity, ε (see Figure 3). The obliquity is the angle between the outer (heliocentric) orbit and inner (mutual) orbit planes. We shall refer to the normals to the outer orbit and inner orbit planes of the binary as orbit pole and spin pole, respectively. Assuming that $2001\,QG_{298}$ was observed exactly equator-on in 2003, then the spin pole must lie on the plane perpendicular to the 2003 line of sight (aspect angle $\theta_{2003} = 90°$) and the obliquity is simply the sky-projected angle between spin pole and the normal to the ecliptic. [Note: The Earth is less than $(1\,\mathrm{AU}/31\,\mathrm{AU})\,(180°/\pi) \approx 1.8°$ away from the orbit plane of

$2001\,QG_{298}$ as seen from the KBO, which is negligible.] In this configuration, the lightcurve has the same shape independent of the obliquity. In 2010 the spin pole of $2001\,QG_{298}$ makes an angle with the line of sight $\theta_{2010} = \arccos(-\sin\varepsilon\,\sin\Delta\nu)$ where $\Delta\nu = 16^\circ$ is the angle through which $2001\,QG_{298}$ has moved along its orbit since 2003. The 2010 aspect angle can take values in the range $90^\circ \leq \theta_{2010} \leq 90^\circ + 16^\circ$ depending on its obliquity[1]. In other words, the equator of $2001\,QG_{298}$ lies at most 16° from the line of sight in 2010.

We took the two models in Table 3 and rendered them as they would appear from Earth in 2010 (Figure 4) following the procedure in LJ07. The resulting 2010 model lightcurves are shown in Figure 5. As expected, at obliquity $\varepsilon = 0^\circ$ the lightcurve displays no change in photometric range, $\Delta m_{2003} = \Delta m_{2010}$. However, the lightcurve phase is shifted (delayed) by $16^\circ/360^\circ \approx 0.044$ as the object must rotate an extra 16° in order to appear at the same rotational phase as seen from Earth. As the obliquity increases, the 2010 photometric range decreases, down to a minimum of $\Delta m_{2010} \sim 0.7$ mag for $\varepsilon = 90^\circ$. The rotational phase shift also decreases as ε increases and for $\varepsilon = 90^\circ$ the shift is zero and the 2003 and 2010 lightcurves appear in phase. As the obliquity approaches $\varepsilon = 90^\circ$ the 2010 lightcurve looks nearly identical for the lunar- and icy-type surfaces. This occurs because the minimum cross-section configuration becomes less affected by limb darkening effects (see Figure 4).

Figure 6 shows how the observed 2003 and 2010 photometric ranges for $2001\,QG_{298}$ compare with the model predictions. Figure 7 overplots our 2010 data on the model lightcurves from Figure 5. The first point to notice is that the new data are consistent with and support the idea advanced by SJ04 that $2001\,QG_{298}$ is a contact binary (or at least a very elongated object), now being observed at a slightly more pole-on geometry than in 2003. Secondly, we find that the new data are inconsistent with a low obliquity. In fact, the data points with smaller error bars are best explained by an obliquity $\varepsilon = 90^\circ$, both in rotational phase and photometric range (Figure 7). We find the lowest reduced χ^2 value ($\tilde{\chi}^2 = 1.7$) for the $\varepsilon = 90^\circ$ model. Since a unit increase from the minimum reduced χ^2 roughly brackets a 1-σ confidence interval (Press et al. 1992), our data suggest an uncertainty in the obliquity smaller than $\Delta\varepsilon = \pm 30^\circ$ (see Table 4). This estimate neglects the effect of the uncertainty in the spin period and rotational phase mentioned in Section 3.1. To address this issue, we used a Monte Carlo simulation that combines the photometric and timing uncertainties. The goal is to quantify the probability that our data are best explained by a given obliquity range. We generated 1000 replicas of the 2010 lightcurve and shifted each by a random phase

[1]Note that we are considering the case (shown as thick solid vectors in Figure 3) in which the pole vector moves away from the observer between 2003 and 2010; the opposite case in which the pole moves towards (and $90^\circ - 16^\circ \leq \theta_{2010} \leq 90^\circ$) the observer (thin dashed vectors in Figure 3) produces a similar effect on the 2010 lightcurve.

drawn from a normal distribution with zero mean and standard deviation 0.06 (see Section 3.1). Then, each replicated data point was nudged independently in the vertical (magnitude) direction by a random amount taken from a normal distribution with zero mean and standard deviation equal to its error bar. We found that 58% of the artificial lightcurves are best explained (in terms of χ^2) by the model with $\varepsilon = 90°$. These are followed by the $\varepsilon = 75°$ model with 12%. We conclude that 70% of the artificial lightcurves sampling the uncertainty region are best explained by models with obliquities in the range $\varepsilon = 90° \pm 30°$. Finally, Figure 8 shows that for $\varepsilon = 90°$ both surface types considered in LJ07 produce similar results implying that the 2010 data are not adequate for discriminating between the two. We conclude that the 2003 and 2010 lightcurves are simultaneously explained by a single contact binary model with large obliquity, $\varepsilon = 90° \pm 30°$. The simultaneous fit is shown in Figure 10.

4. Discussion

The large obliquity of contact binary KBO $2001\,\mathrm{QG}_{298}$ is not unusual; it is a property that is shared by other extreme shape objects in the solar system. Table 5 lists the subset of bodies from the Planetary Data System asteroid lightcurve database (Warner et al. 2009) with maximum photometric variability larger than $\Delta m = 0.9$ mag (indicative of extreme shapes) and effective diameter larger than $D_\mathrm{e} = 100$ km. We have ignored smaller objects as they were probably more strongly affected by collisions and non-gravitational effects that could interfere with their spins. The bodies in Table 5 are well studied and known to have extreme shapes, and they all have obliquities in the range $50° < \varepsilon < 180° - 50°$. Although suggestive, the obliquities of the objects in Table 5 are nonetheless consistent with an isotropic distribution. Randomly oriented spin poles fall in that same range of obliquities with probability $p = \cos 50° = 0.64$. Hence, the chance that all four objects in Table 5 fall in that range, $p^4 = 0.17$, remains high. The sample size is too small to draw definite conclusions.

The origin of contact binaries remains unexplored. KBO binary formation theories have focussed on the more easily identified resolved pairs (Weidenschilling 2002; Goldreich et al. 2002; Funato et al. 2004; Astakhov et al. 2005; Schlichting & Sari 2008a; Nesvorný et al. 2010). The general idea behind wide-binary formation models is to identify a mechanism that removes energy from a close but unbound pair of KBOs, converting it into a gravitationally bound binary. Contact binaries are perhaps an end state of initially "hard" (binding energy of the binary larger than the mean kinetic energy of single objects) wide-binaries that have been progressively further hardened by close encounters with passing, single bodies (Heggie

1975; Goldreich et al. 2002). Recently, Perets & Naoz (2009) proposed a contact binary formation mechanism based on the combined effects of Kozai oscillations and tidal friction.

Kozai oscillations (Kozai 1962; Fabrycky & Tremaine 2007) occur in hierarchical triple systems (the Sun and the KBO binary in this case) with large mutual orbital inclinations. In the solar system, the mutual inclination between the inner and outer orbits of a binary is by definition the obliquity, ε. If the initial obliquity ε_0 is larger than the Kozai critical angle, typically $\varepsilon_c \approx 40^\circ$, the binary orbital eccentricity and obliquity will oscillate in an anti-correlated fashion. As the obliquity falls to a minimum of $\varepsilon = 0^\circ$ the eccentricity attains its maximum value which depends on ε_0 and approaches unity for $\varepsilon_0 \approx 90^\circ$. Such large eccentricities will bring the binary components very close (possibly even leading to collisions) allowing tidal friction to dissipate energy and gradually shrink the binary semimajor axis. Perets & Naoz (2009) propose that repeated episodes of Kozai oscillations and tidal friction could eventually lead to very compact systems – possibly contact binaries or highly elongated objects – with eccentricities $e \approx 0$ and inclinations $40^\circ < \varepsilon_0 < 180^\circ - 40^\circ$.

4.1. The fraction of contact binaries revisited

Current estimates of the intrinsic fraction of contact binaries among the Jupiter Trojans and the KBOs assume that their spins are isotropically oriented (LJ07; Mann et al. 2007). Since contact binaries are identified from their high variability only if observed at an aspect angle sufficiently close to $\theta = 90^\circ$, the apparent fraction must be corrected for the probability of such favorable viewing geometry. LJ07 find minimum aspect angles for positive contact binary identification of $\theta_{\rm lunar} = 81^\circ$ and $\theta_{\rm icy} = 71^\circ$ for lunar- and icy-type surfaces, respectively. The probability that a randomly oriented contact binary is observed at aspect angle $\theta > \theta_{\rm min}$ is given by $\cos\theta_{\rm min}$ (Lacerda & Luu 2003) and amounts to $p_{\rm lunar} = \cos 81^\circ = 0.15$ and $p_{\rm icy} = \cos 71^\circ = 0.33$ for the extreme surface types considered. Based on the discovery of $2001\,{\rm QG}_{298}$ in a sample of 34 KBOs (see SJ04), LJ07 calculate lower limits to the fraction of contact binaries of $f_{\rm lunar} > 20\%$ or $f_{\rm icy} > 9\%$ depending on the assumed scattering law.

The estimated abundance will be higher if most contact binaries have high obliquities. Figure 10 illustrates the solid angle region available to spin poles with high obliquities, in the range $40^\circ < \varepsilon < 180^\circ - 40^\circ$, and the fraction of that region detectable from Earth. We numerically integrated the "detectable" and "allowed" solid angles and found their ratio (which equals the detection probability) to be $p'_{\rm lunar} = 0.11$ and $p'_{\rm icy} = 0.24$ for the two surface types. The lower detection probabilities with respect to the isotropic case imply larger intrinsic abundances by $0.15/0.11 = 36\%$ (lunar scattering) and $0.33/0.24 = 38\%$ (icy scattering). Therefore, if contact binaries have obliquities in the range shown in Figure 10

then the lower limit abundance would increase to $f_{\rm lunar} > 27\%$, assuming lunar-scattering, and $f_{\rm icy} > 12\%$, assuming icy scattering.

5. Conclusions

We have measured the visible lightcurve of Kuiper belt object 2001 QG_{298} and compared it to similar data collected in 2003. Our findings can be summarised as follows:

1. The 2010 lightcurve of 2001 QG_{298} has a peak-to-peak range of $\Delta m_{2010} = 0.7 \pm 0.1$ mag, significantly lower than the photometric range in 2003, $\Delta m_{2003} = 1.14 \pm 0.04$ mag. The 2003 and 2010 lightcurves appear in phase when shifted by an integer number of full rotations.

2. The change between the 2003 and 2010 lightcurves is most simply explained if 2001 QG_{298} possesses a large obliquity, $\varepsilon = 90^\circ \pm 30^\circ$. In that case, the lightcurve photometric range should continue to decrease, reaching a minimum of $\Delta m \sim 0.0 - 0.1$ mag in 2049.

3. Current estimates of the fraction of contact binaries in the Kuiper belt assume that these objects have randomly oriented spins. If, as 2001 QG_{298}, contact binaries tend to have large obliquities their abundance may be larger than previously believed.

Acknowledgments

I thank David Jewitt for carefully reading and reviewing the manuscript. I also thank Hilke Schlichting, Henry H. Hsieh and Maaike van Vlijmen for helpful comments, and Alan Fitzsimmons for useful discussions. Hugo Lacerda Cruz and K. de Koek assisted in the preparation of the manuscript. I am very grateful for the financial support from a Michael West Research Fellowship and from the Royal Society in the form of a Newton Fellowship. I thank James McCormac for a thorough tour of the Isaac Newton Telescope. The observations presented in this paper were obtained as part of the Isaac Newton Group observing program I/2010B/15.

REFERENCES

Astakhov, S. A., Lee, E. A., & Farrelly, D. 2005, MNRAS, 360, 401

Benecchi, S. D., Noll, K. S., Grundy, W. M., Buie, M. W., Stephens, D. C., & Levison, H. F. 2009, Icarus, 200, 292

Bernstein, G. M., Trilling, D. E., Allen, R. L., Brown, M. E., Holman, M., & Malhotra, R. 2004, AJ, 128, 1364

Booth, M., Wyatt, M. C., Morbidelli, A., Moro-Martín, A., & Levison, H. F. 2009, MNRAS, 399, 385

Chandrasekhar, S. 1963, ApJ, 138, 1182

Cruikshank, D. P., Dalle Ore, C. M., Roush, T. L., Geballe, T. R., Owen, T. C., de Bergh, C., Cash, M. D., & Hartmann, W. K. 2001, Icarus, 153, 348

de Angelis, G. 1995, Planet. Space Sci., 43, 649

Descamps, P., et al. 2011, Icarus, 211, 1022

—. 2009, Icarus, 203, 102

Detal, A., Hainaut, O., Pospieszalska-Surdej, A., Schils, P., Schober, H. J., & Surdej, J. 1994, A&A, 281, 269

Dunlap, J. L., & Gehrels, T. 1969, AJ, 74, 796

Fabrycky, D., & Tremaine, S. 2007, ApJ, 669, 1298

Fraser, W. C., et al. 2008, Icarus, 195, 827

Fuentes, C. I., & Holman, M. J. 2008, AJ, 136, 83

Funato, Y., Makino, J., Hut, P., Kokubo, E., & Kinoshita, D. 2004, Nature, 427, 518

Gnat, O., & Sari, R. 2010, ApJ, 719, 1602

Goldreich, P., Lithwick, Y., & Sari, R. 2002, Nature, 420, 643

Grundy, W. M., et al. 2011, Icarus, doi:10.1016/j.icarus.2011.03.012

Hartmann, W. K., & Cruikshank, D. P. 1978, Icarus, 36, 353

Heggie, D. C. 1975, MNRAS, 173, 729

Jewitt, D. C., & Luu, J. X. 1995, AJ, 109, 1867

Kenyon, S. J., & Luu, J. X. 1998, AJ, 115, 2136

Kern, S. D., & Elliot, J. L. 2006, ApJ, 643, L57

Kozai, Y. 1962, AJ, 67, 591

Kryszczyńska, A., La Spina, A., Paolicchi, P., Harris, A. W., Breiter, S., & Pravec, P. 2007, Icarus, 192, 223

Lacerda, P. 2008, ApJ, 672, L57

Lacerda, P., & Jewitt, D. C. 2007, AJ, 133, 1393

Lacerda, P., & Luu, J. 2003, Icarus, 161, 174

Leone, G., Paolicchi, P., Farinella, P., & Zappala, V. 1984, A&A, 140, 265

Mann, R. K., Jewitt, D., & Lacerda, P. 2007, AJ, 134, 1133

Michałowski, T., Colas, F., Kwiatkowski, T., Kryszczyńska, A., Hirsch, R., & Michałowski, J. 2001, A&A, 378, L14

Murray-Clay, R. A., & Schlichting, H. E. 2011, ApJ, 730, 132

Nesvorný, D., Vokrouhlický, D., Bottke, W. F., Noll, K., & Levison, H. F. 2011, AJ, 141, 159

Nesvorný, D., Youdin, A. N., & Richardson, D. C. 2010, AJ, 140, 785

Noll, K. S., Grundy, W. M., Stephens, D. C., Levison, H. F., & Kern, S. D. 2008, Icarus, 194, 758

Noll, K. S., et al. 2002, AJ, 124, 3424

Perets, H. B., & Naoz, S. 2009, ApJ, 699, L17

Petit, J.-M., & Mousis, O. 2004, Icarus, 168, 409

Press, W. H., Teukolsky, S. A., Flannery, B. P., & Vetterling, W. T. 1992, Numerical Recipes in FORTRAN: The Art of Scientific Computing, 2nd edn. (New York, NY, USA: Cambridge University Press)

Schlichting, H. E., & Sari, R. 2008a, ApJ, 673, 1218

—. 2008b, ApJ, 686, 741

Sheppard, S. S., & Jewitt, D. 2004, AJ, 127, 3023

Sheppard, S. S., & Jewitt, D. C. 2002, AJ, 124, 1757

Smith, J. A., et al. 2002, AJ, 123, 2121

Stansberry, J. A., Grundy, W. M., Margot, J. L., Cruikshank, D. P., Emery, J. P., Rieke, G. H., & Trilling, D. E. 2006, ApJ, 643, 556

Stephens, D. C., & Noll, K. S. 2006, AJ, 131, 1142

Takahashi, S., & Ip, W.-H. 2004, PASJ, 56, 1099

Trujillo, C. A., Jewitt, D. C., & Luu, J. X. 2001, AJ, 122, 457

Warner, B. D., Harris, A. W., & Pravec, P. 2009, Icarus, 202, 134

Weidenschilling, S. J. 1980, Icarus, 44, 807

—. 2002, Icarus, 160, 212

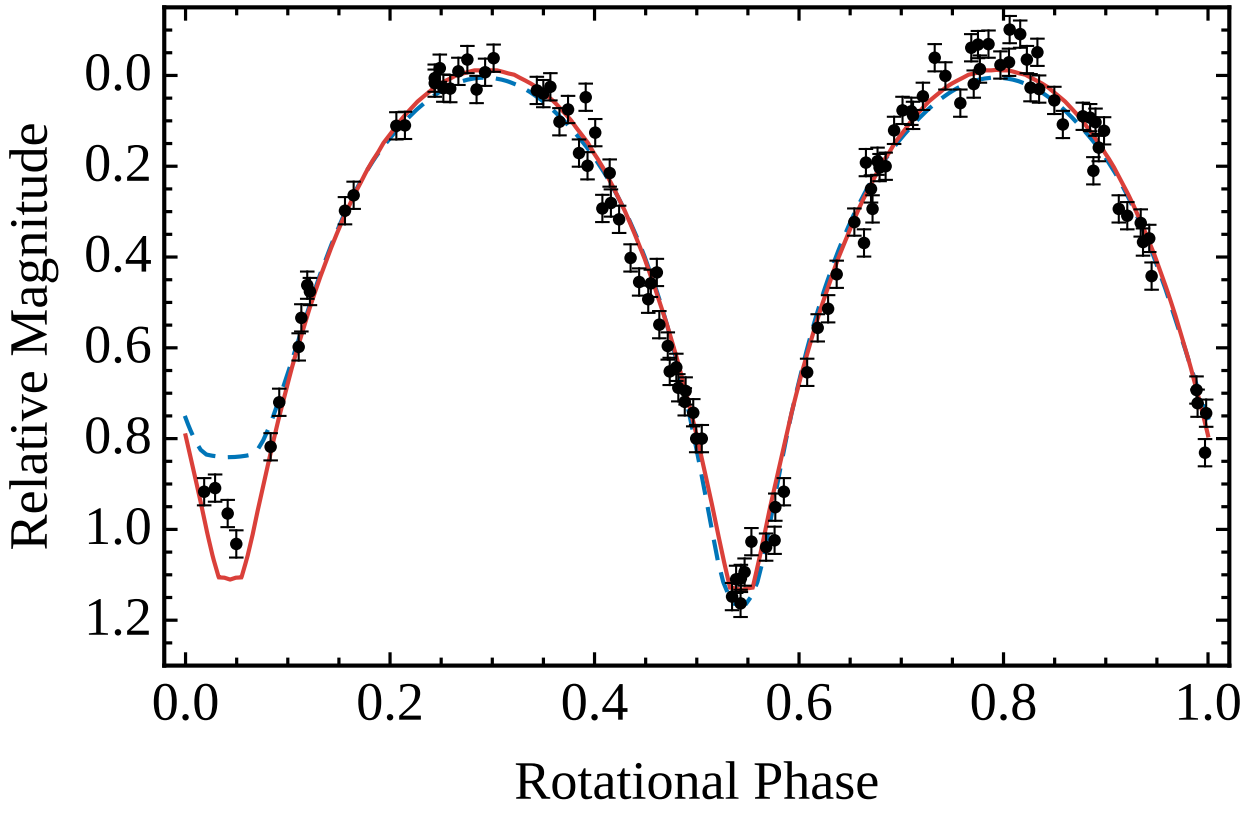

Fig. 1.— KBO 2001 QG_{298} lightcurve data (black points) obtained in 2003 by Sheppard & Jewitt (2004). Fits based on Roche binaries are shown as solid lines (Lacerda & Jewitt 2007). Blue (dashed) line assumes an icy-type surface and red (solid) line assumes a lunar-type surface. The model binaries are rendered in Fig. 4.

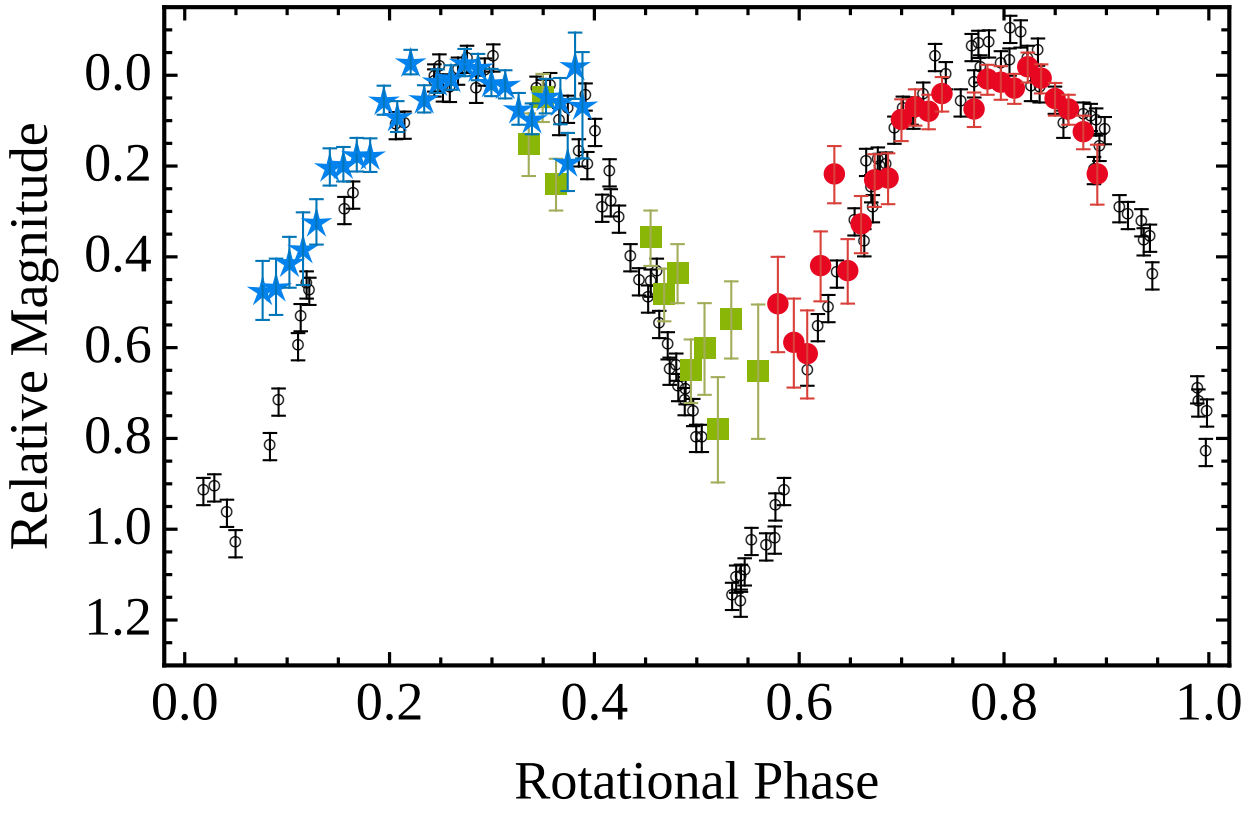

Fig. 2.— Lightcurves of KBO 2001 QG_{298} in 2003 (open circles; Sheppard & Jewitt 2004) and 2010 (filled symbols; this work). Red circles, green squares and blue stars indicate data from 2010 August 15, 16 and 17, respectively. The photometric range has decreased from $\Delta m_{2003} = 1.14 \pm 0.04$ mag in 2003 to $\Delta m_{2010} = 0.7 \pm 0.1$ mag in 2010. The 2003 and 2010 lightcurves appear in phase.

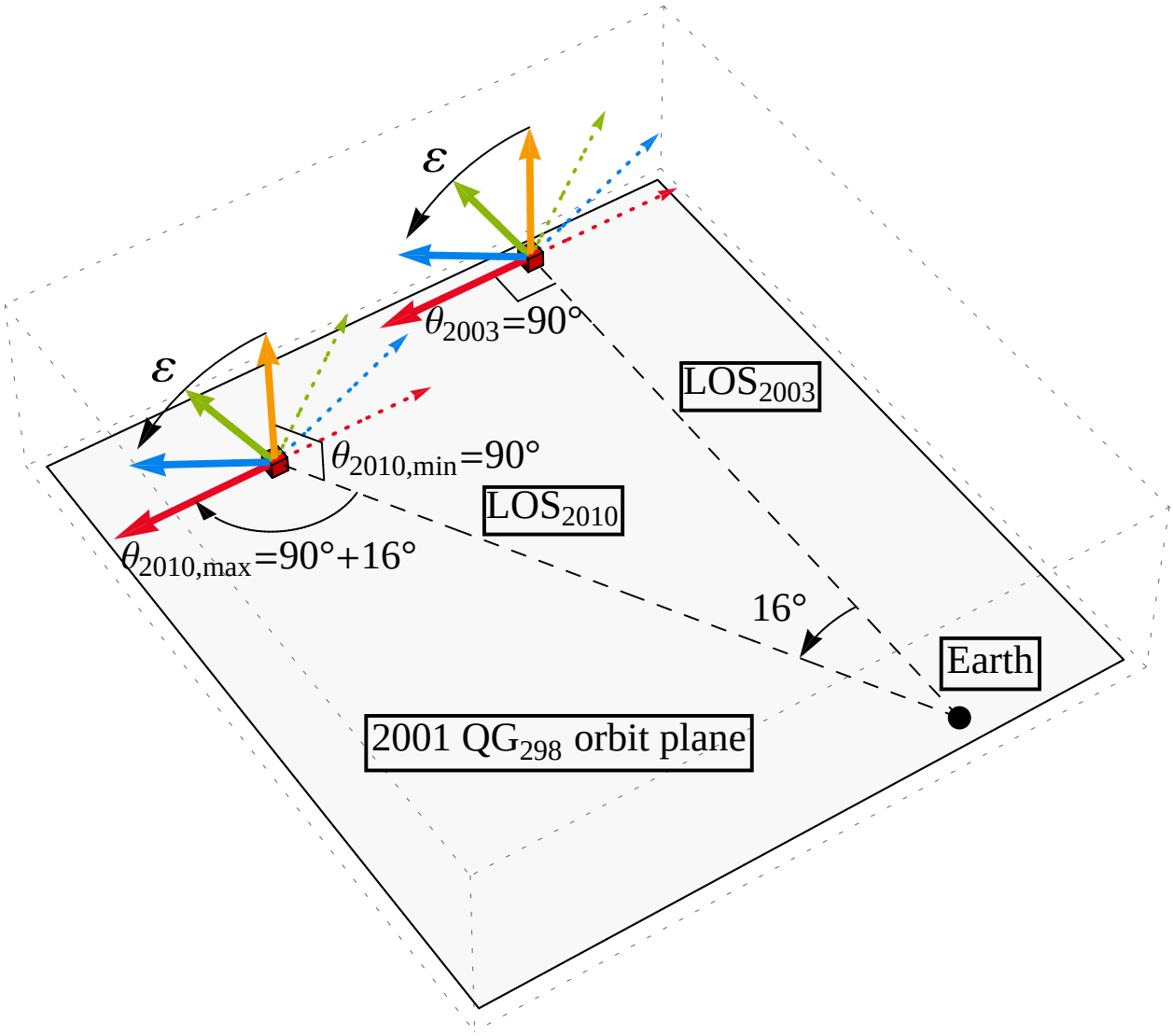

Fig. 3.— Geometric circumstances and relevant angles used to describe the lightcurve observations of 2001 QG_{298} in 2003 and 2010. The orbit plane of 2001 QG_{298} is shaded and labelled. The location of the Earth (black dot) and the lines of sight (dashed lines "LOS_{2003}" and "LOS_{2010}") towards 2001 QG_{298} are also indicated. The positions of 2001 QG_{298} in 2003 and 2010 are marked by red boxes. A few possible spin pole orientations (obliquities $\varepsilon = 0°, 30°, 60°, 90°$ measured from the normal to the orbit plane, as indicated) for 2001 QG_{298} are illustrated as thick solid arrows emerging from the object. Thinner dashed lines correspond to symmetric pole orientations (w.r.t. $\varepsilon = 0°$) which produce similar lightcurves to their counterparts and cannot be observationally distinguished. Under the assumption that the 2003 aspect angle $\theta_{2003} = 90°$, the 2010 aspect angle lies in the range $90° \leq \theta_{2010} \leq 90° + 16°$ (or equivalently $90° - 16° \leq \theta_{2010} \leq 90°$) depending on the obliquity.

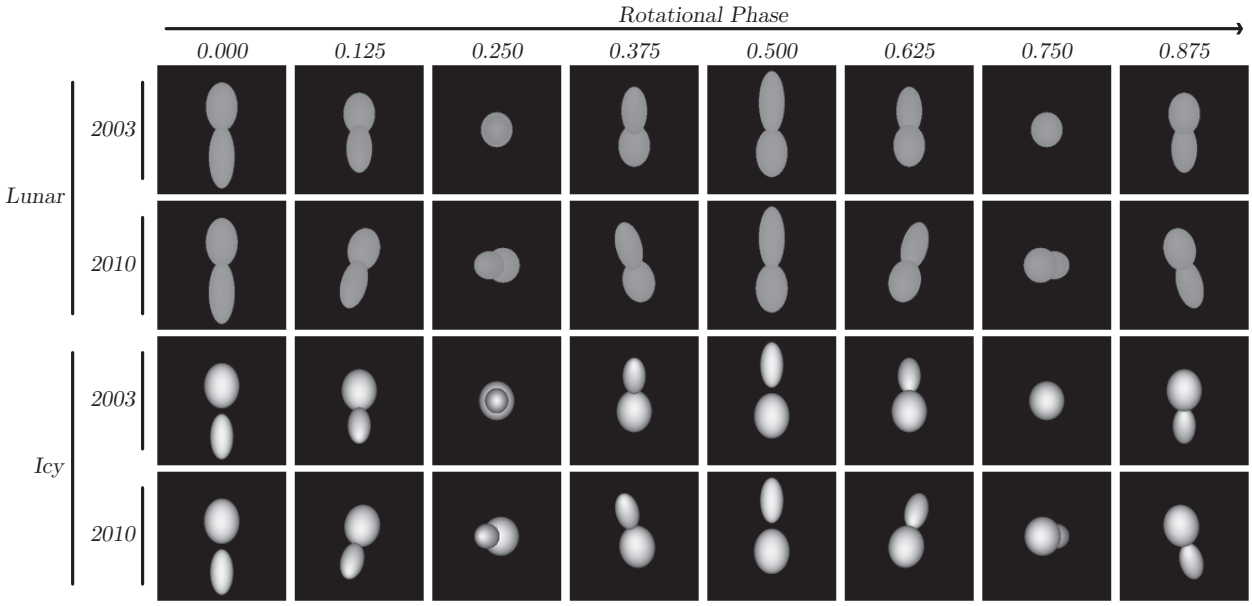

Fig. 4.— Renderings of the Roche binary models of 2001 QG_{298} (Lacerda & Jewitt 2007) assuming lunar-type (top two rows) and icy-type (bottom two rows) surface scattering. The models are rendered as seen from Earth in 2003 (rows 1 and 3 from top) and in 2010 (rows 2 and 4 from top) assuming that 2001 QG_{298} has obliquity $\varepsilon = 90°$. Successive rotational phases are displayed from left to right to simulate rotation and to show maximum and minimum cross-section configurations.

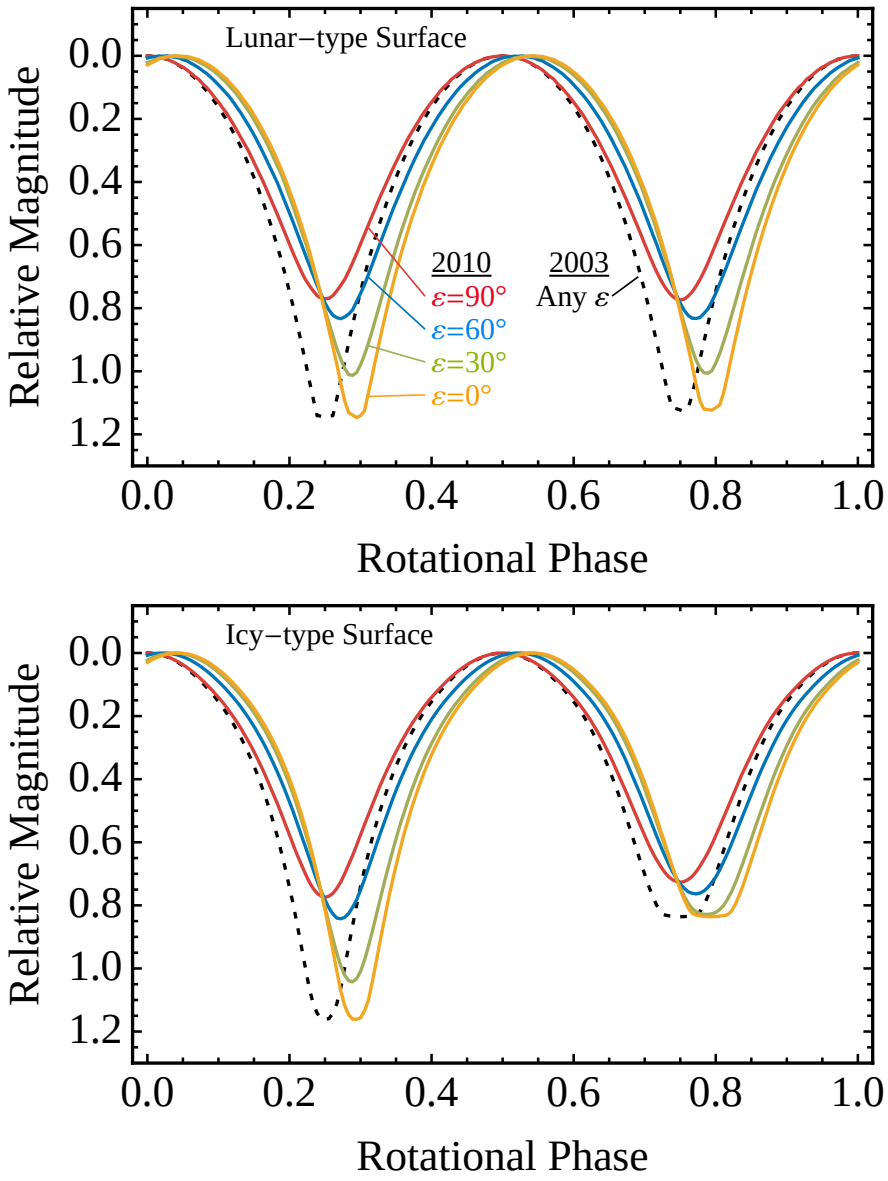

Fig. 5.— 2001 QG_{298} lightcurve model predictions for 2010 (solid, colored lines) based on the 2003 models (dashed lines). The predicted lightcurve range and phase depend on the assumed obliquity ε. Lunar-type (icy-type) scattering models are shown in the top (bottom) panel.

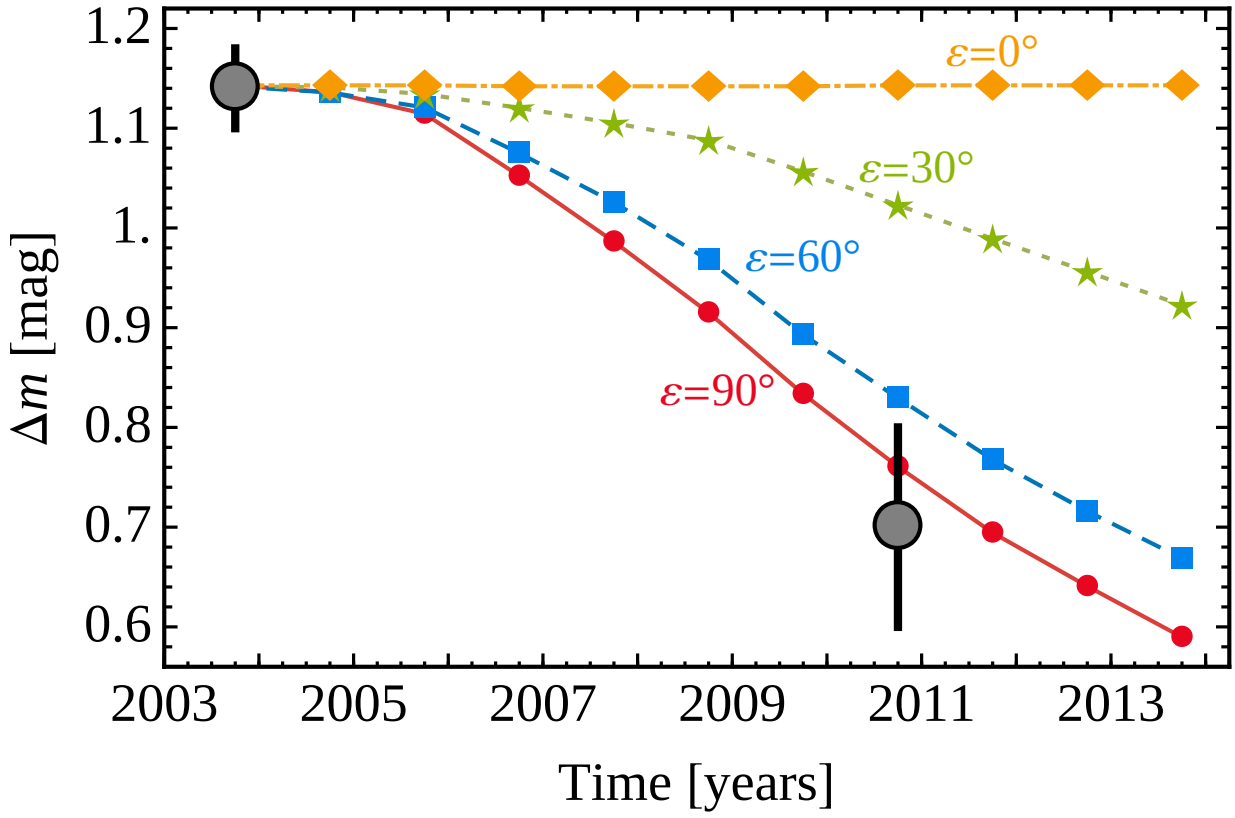

Fig. 6.— Predicted photometric range for 2001 QG_{298} as a function of time and obliquity. Measured 2003 and 2010 photometric ranges are shown as large gray points with 1-σ error bars. Table 4 lists the Δm values as a function of obliquity at the time of the 2010 measurement.

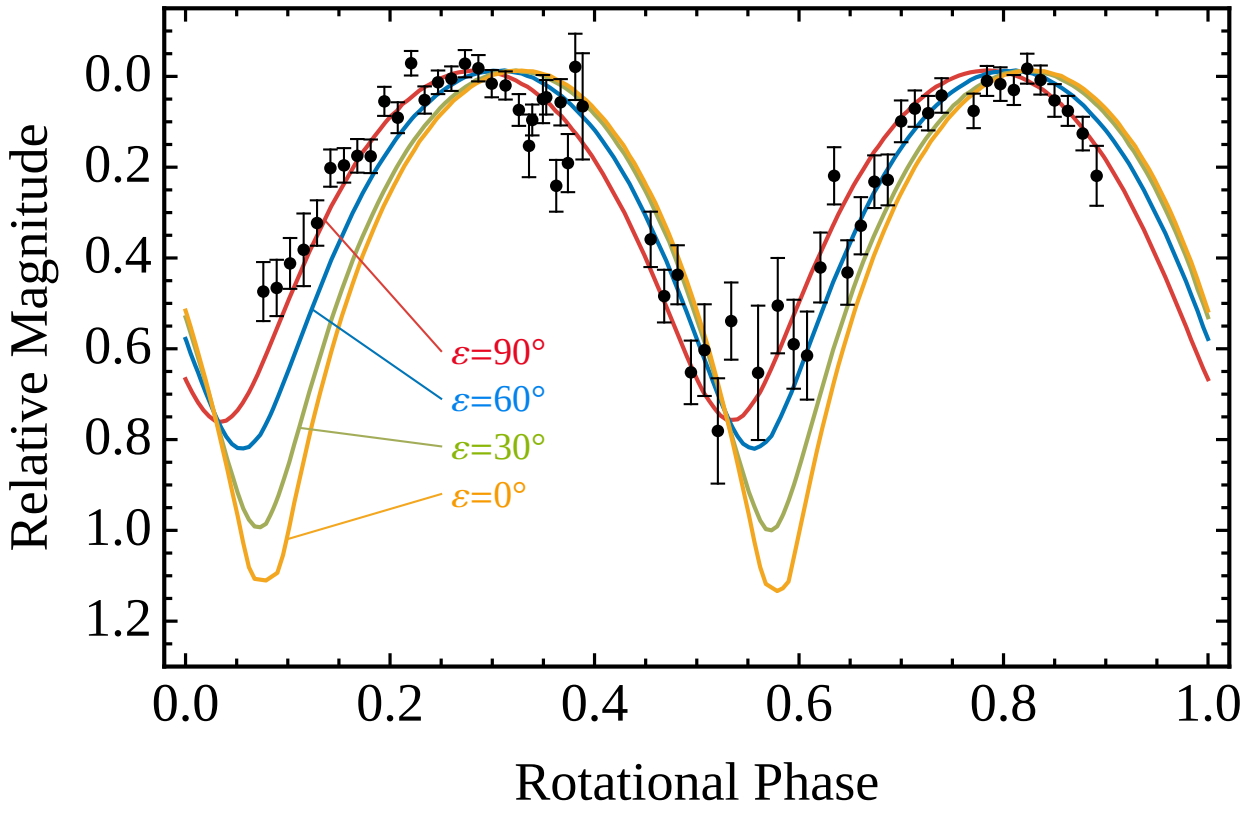

Fig. 7.— Comparison between the 2010 lightcurve data (black dots with error bars) and the model predictions shown in Fig. 5. Only the lunar-type scattering models are plotted. Different lines assume obliquities $\varepsilon = 0°, 30°, 60°, 90°$. Respective reduced χ^2 values for the fits are $\chi^2_{\rm red} = 18.8, 12.3, 4.4, 1.7$, favoring the solution $\varepsilon = 90°$.

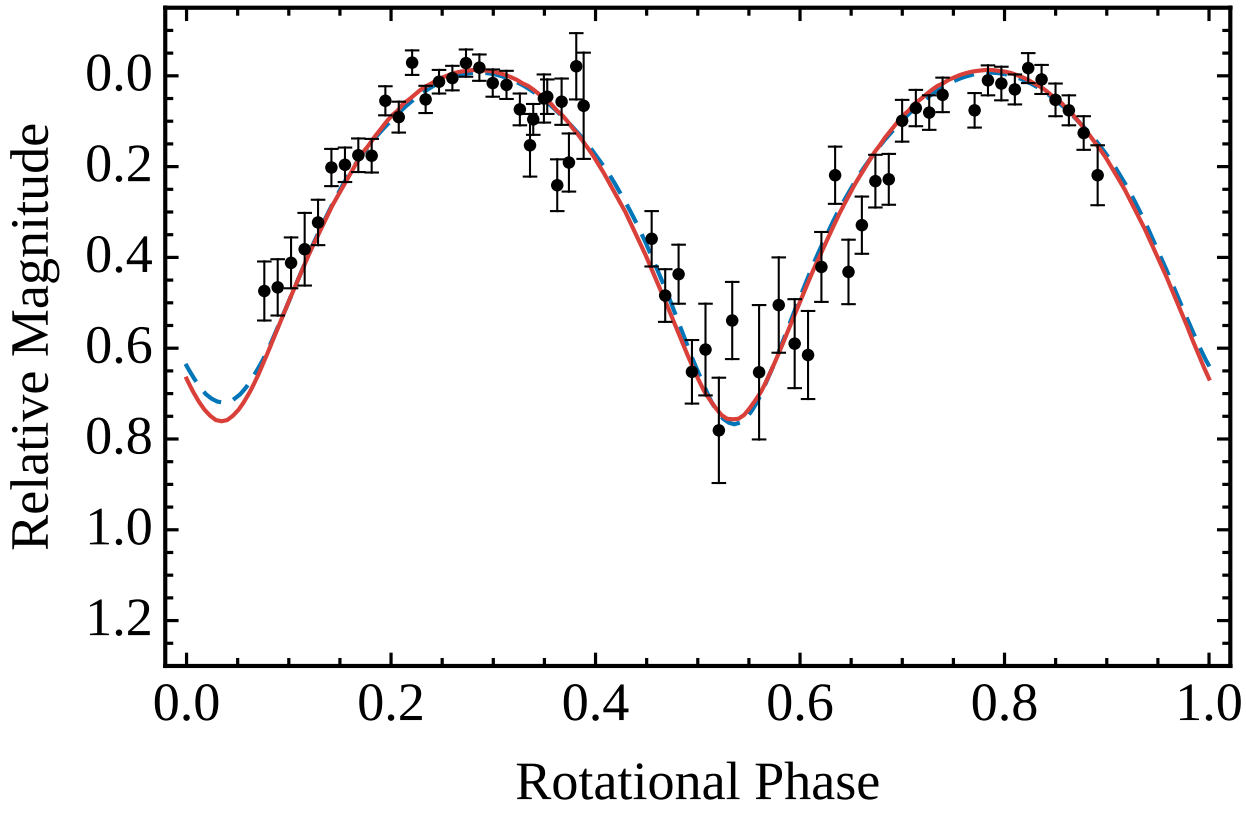

Fig. 8.— Negligible difference between the lunar- (red, solid) and icy-type (blue, dashed) scattering model lightcurves.

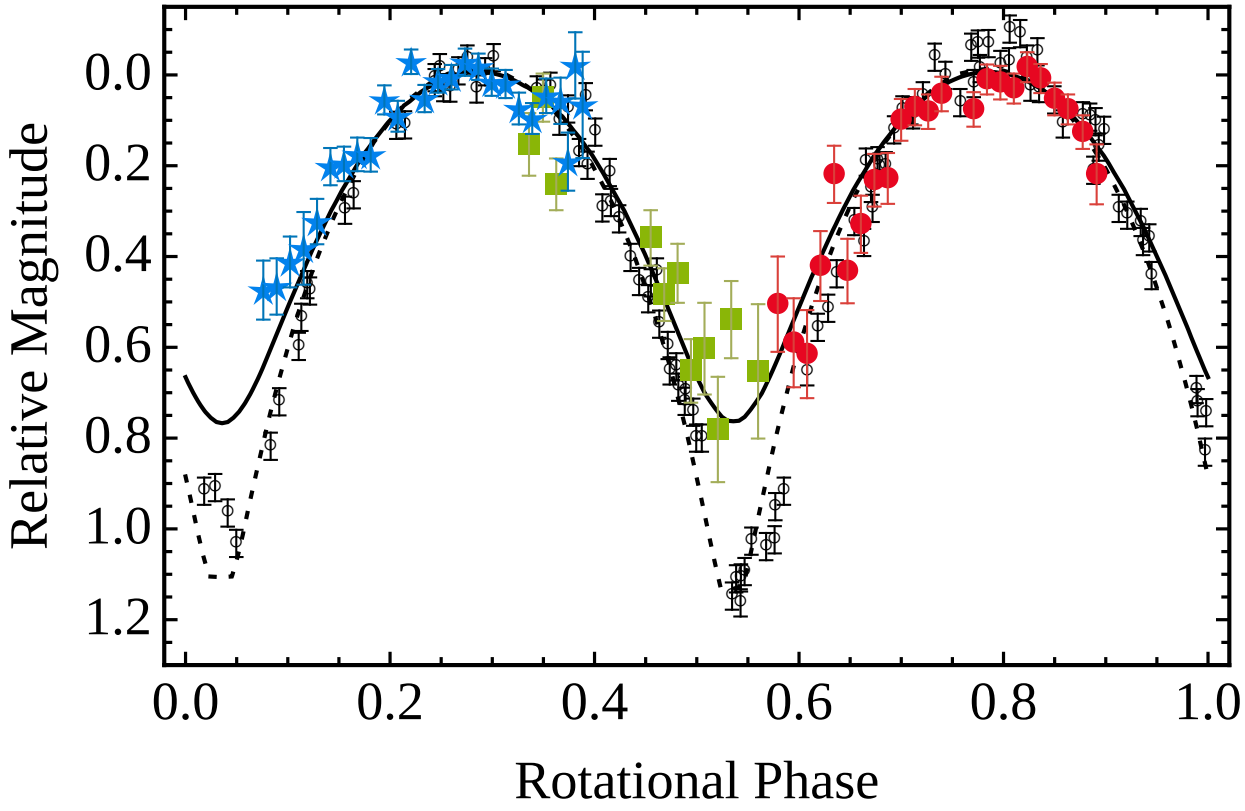

Fig. 9.— Lightcurves from 2003 and 2010 (as shown in Fig. 2) simultaneously fit by the model in Fig. 4 (top two rows). The model assumes obliquity $\varepsilon = 90°$.

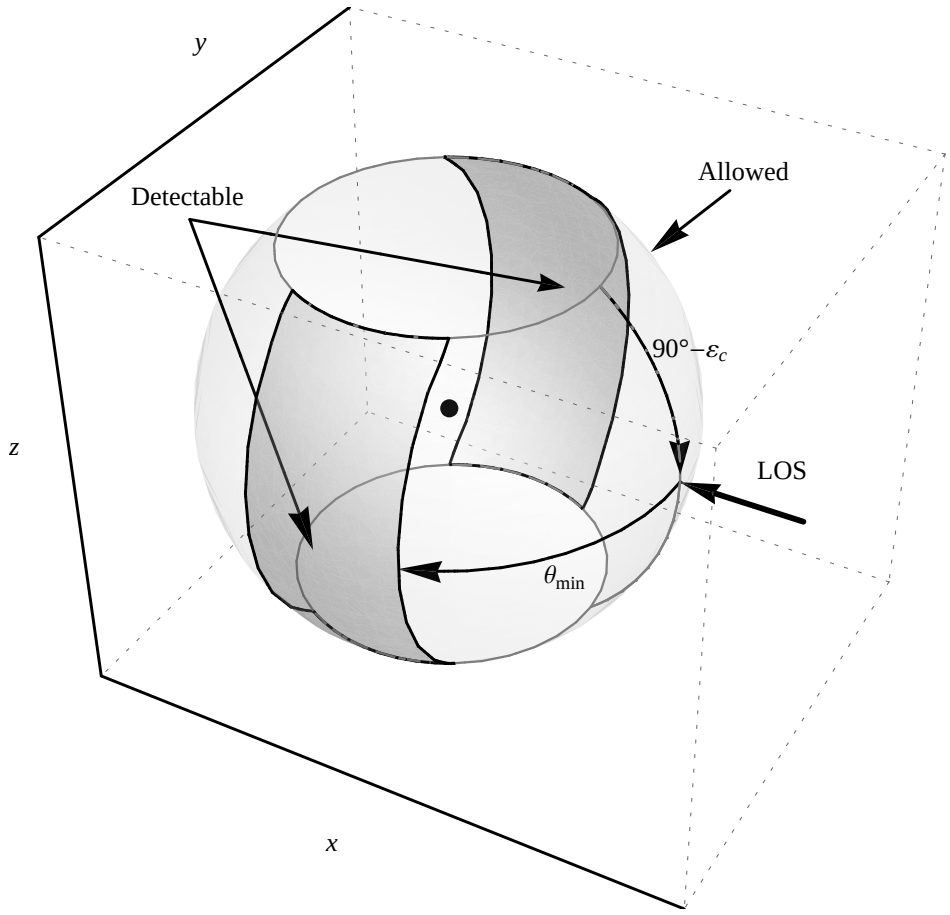

Fig. 10.— Solid angles used to calculate the probability that a contact binary with obliquity in the range $\varepsilon_c < \varepsilon < 180° - \varepsilon_c$ ($\varepsilon_c = 40°$) will be detected from its high photometric variability. The line of sight is indicated by a thick, black arrow labelled "LOS". Solid angle regions of interest are marked on the surface of a sphere surrounding the contact binary (marked by a black dot). The solid angle region where spin poles are allowed with uniform probability is shaded in light gray. That region is defined as the full sphere minus polar caps extending an angle ε_c from the either pole. Darker gray regions mark spin pole orientations that are detectable from Earth. Those regions lie more than $\theta_{\rm min}$ from the LOS. The ratio of these detectable and allowed solid angles equals the detection probability.

Table 1. Journal of Observations.

UT Date	R [a] [AU]	Δ [b] [AU]	α [c] [°]	Filt. [d]	Seeing [e] [″]	Exp. [f] [s]	Notes
2010 Aug 15	31.7618	31.1064	1.41	r	0.9-1.5	600	photometric
2010 Aug 16	31.7618	31.1053	1.41	r	1.3-1.7	600	clouds
2010 Aug 17	31.7618	31.1042	1.41	r	0.9-1.3	600	thin cirrus

Note. — All observations conducted at the 2.5-m Isaac Newton Telescope.

[a]Heliocentric distance in AU;

[b]Geocentric distance in AU;

[c]Phase angle in degrees;

[d]Filters used;

[e]Typical seeing in arcseconds;

[f]Typical integration time per frame in seconds.

Table 2. Calibration Stars.

SDSS Name	r [a] [mag]	$g-r$ [b] [mag]
SDSS J005028.45+020005.7	18.473 ± 0.016	1.39
SDSS J005023.64+015726.9	18.951 ± 0.025	1.22
SDSS J005026.24+015716.2	17.528 ± 0.024	0.56
SDSS J005012.65+015638.6	19.131 ± 0.026	1.32
SDSS J005011.82+015538.0	17.932 ± 0.024	0.97

[a]SDSS PSF r magnitude;

[b]SDSS Model $g-r$ color;

Table 3. $2001\,\mathrm{QG}_{298}$ models.

Surface [a]	q [b]	B/A [c]	C/A [c]	b/a [d]	c/a [d]	$\omega^2/(\pi\,G\,\rho)$ [e]	$d/(A+a)$ [f]	ρ [g]
Lunar	0.84	0.72	0.65	0.45	0.41	0.130	0.90	0.59
Icy	0.44	0.85	0.77	0.53	0.49	0.116	1.09	0.66

[a]Surface scattering type;

[b]Mass ratio of the binary components;

[c]Axis ratios of primary;

[d]Axis ratios of the secondary;

[e]Dimensionless spin frequency of triaxial binary;

[f]Dimensionless binary orbital separation;

[g]Bulk density of the models (in g cm^{-3}).

Table 4. Model Goodness of Fit.

	Model Photometric Range [b]		
Obliquity [a]	Δm_{03} [mag]	Δm_{10} [mag]	$\chi^2_{\rm red}$ [c]
$\varepsilon = 90°$	1.14	0.77	1.7
$\varepsilon = 75°$	1.14	0.79	2.4
$\varepsilon = 60°$	1.14	0.83	4.4
$\varepsilon = 45°$	1.14	0.91	7.7
$\varepsilon = 30°$	1.14	1.02	12.3
$\varepsilon = 15°$	1.14	1.13	16.9
$\varepsilon = 0°$	1.14	1.14	18.8

[a]Obliquity of the model;

[b]Model photometric ranges in 2003 and 2010 assuming lunar-type scattering;

[c]Reduced χ^2 value of 2010 model fit to the 2010 lightcurve.

Table 5. Objects with Extreme Shapes.

Name [a]	Group [b]	D_e [c] [km]	P [d] [hr]	Δm_{max} [e] [mag]	Obliquity [f] [°]	Shape [g]	Refs.
90 Antiope	MBA	120	16.5	0.90	53 ± 2	Close binary	1,2
216 Kleopatra	MBA	135	5.4	1.20	84 ± 2	Bi-lobed	3,4,5
624 Hektor	Trojan	230	6.9	1.10	98 ± 5	Contact binary	3,4,6,7
139775 2001 QG_{298}	KBO	250	13.8	1.14	90 ± 30	Contact binary	7,8,9

References. — (1) Michałowski et al. (2001); (2) Descamps et al. (2009); (3) de Angelis (1995); (4) Kryszczyńska et al. (2007); (5) Descamps et al. (2011); (6) Dunlap & Gehrels (1969); (7) Lacerda & Jewitt (2007); (8) Sheppard & Jewitt (2004); and (9) this work.

[a]Object designation;

[b]Object group (MBA=main-belt asteroid, Trojan=Jupiter Trojan, KBO=Kuiper belt object;

[c]Effective diameter;

[d]Approximate spin period;

[e]Maximum observed photometric range;

[f]Approximate obliquity.

[g]Most probable shape.